

Response Letter

Dear Editor,

Please find below our point by point response to your remarks. We want to apologise that some of these points could have been already treated by us in the previous round of revision. For that reason we are even more thankful that you gave us the chance responding to them now.

We hope that the revisions that we performed accordingly are satisfactory and that the manuscript can be considered for publication in Biogeosciences.

Sincerely,

Andreas Hartmann on behalf of the co-authors.

Point by point response

Comment 1: *In your response to the question regarding DOC and DIN methods, some years are indicated as “xxxxx” instead of a specific year. Please, correct. Also, this paragraph is too long and very difficult to read; you can just provide the type/material and pore-size of the filters; it is not necessary to mention the company and/or catalogue number (e. g, MILLIPOR HTTP04700). Please, revise.*

Response: Thanks for this valuable comment. The unnecessary information was removed to make the paragraph easier to read. Only the devices for analysis were left (lines 115-121 in the re-revised manuscript).

Comment 2: *Comment 5 by Reviewer #2 is not adequately addressed. “Could the impact be hidden by soil buffering effect or variations in the hydrological connectivity (e.g.: if less ET and less interception would induce more infiltration and deeper flowpaths through layers that would be poorer in DOC?) “. Could you please discuss in more detail in the manuscript? Also, in the response (lines 379-385), it is mentioned “these superficial changes are probably minor considering... ” I would suggest revising to “these changes are probably minor considering...”*

Response: We admit that we missed to specifically answer to this question. Indeed some changes on DOC availability and leaching may be hidden. We added

“Consequently, a disturbance caused impact on DOC availability could also be hidden because increased infiltration and DOC leaching during strong rainfall events may just not be detectable considering the weekly to monthly sampling of DOC. “

to lines 375-378 in the re-revised manuscript.

Comment 3: *In response to Comment #14, you mention that “For both, disturbance induced changes of DOC and hydrological processes, more sampling in high temporal-resolution should be undertaken*

to elucidate the effect of forest disturbance within the studied ecosystem.” Can you please indicate which parameters need to be measured at high spatial resolution (e.g., DOC, DIN NH₄⁺, other?) and for which aspects of the model (e.g., calibration, evaluation, other?) this would be critical?

Response: We specified the recommendation to

“For a better understanding of disturbance induced changes of DOC, more sampling in high temporal-resolution of DOC concentrations at the weir (Figure 1) should be undertaken to elucidate the effect of forest disturbance on DOC dynamics and to improve the simulation of DOC production and transport within the studied ecosystem.”

in lines 378-381 in the re-revised manuscript.

Comment 4: *Response to comment #15 is not clear. The sentence ““more than two times 2 mg/l than the pre-disturbance value” is still not clear, please revise.*

Response: The confusing sentence was rephrased to be understandable now:

“Its parameter values showed a production rate P_{DIN} of DIN almost 2 mg/l larger than the pre-disturbance value, an amplitude A_{DIN} around 1 mg/l smaller, and a phase shift $S_{PH,DIN}$ towards a week earlier in the year, resulting in a more acceptable simulation of DIN dynamics during the disturbance period (Figure 7).”

We apologise for missing this one in the first round of the review. See lines 288-291 in the re-revised manuscript.

Comment 5: *Some of the points discussed in your response to comments #16 and #19 are not adequately captured in the revised text in lines 379-385. Can you please revise the text accordingly to capture your response to Reviewer’s 2 technical comments #16 and #19?*

Response: Thanks for this valuable comment. In lines 404-410 of the original manuscript we already provided a discussion on comment 16 of reviewer #2:

“The apparent shift of $S_{PH,DIN}$ towards an earlier maximum of DIN release (7 days) is most probably be due to the earlier onset of snow melt in open areas as compared to forests because snow melt is a major driver of DIN leaching from the soils in our study area (Jost et al., 2010). However, due to the rather slow melting rates, most of the melting water will slowly/diffusively enter the groundwater system rather than flowing rapidly through the karst conduits. Therefore, a slightly earlier beginning of snowmelt may not be visible at the system outlet due to the slow reaction of the groundwater storage.”

Concerning a more detailed answer on comment 19 of reviewer #2 we added

“Therefore, hydrological impacts of windthrow on karst systems (for instance on transpiration) may not be as pronounced as in non-karstic domains because a large fraction of the infiltration during high flow periods will not be available for transpiration anyway.”

to the elaborations on comments 2 and 3 of the editor (lines 372-375 of the re-revised manuscript).

Below: Re-revised version of the manuscript with changes tracked

1 **Model aided quantification of dissolved carbon and**
2 **nitrogen release after windthrow disturbance in an Austrian**
3 **karst system**

4
5 **A. Hartmann^{1,2}, J. Kobler³, M. Kralik³, T. Dirnböck³, F. Humer³ and M. Weiler¹**

6 [1] Faculty of Environment and Natural Resources, Freiburg University, Germany

7 [2] Department of Civil Engineering, University of Bristol, UK

8 [3] Environment Agency Austria, Vienna, Austria

9 Correspondence to: A. Hartmann (andreas.hartmann@hydrology.uni-freiburg.de)

10

11 **Abstract**

12 Karst systems are important for drinking water supply. Future climate projections indicate
13 increasing temperature and a higher frequency of strong weather events. Both will influence
14 the availability and quality of water provided from karst regions. Forest disturbances such as
15 windthrow can disrupt ecosystem cycles and cause pronounced nutrient losses from the
16 ecosystems. In this study, we consider the time period before and after the wind disturbance
17 period (2007/08) to identify impacts on DIN (dissolved inorganic nitrogen) and DOC
18 (dissolved organic carbon) with a process-based flow and solute transport simulation model.
19 Calibrated and validated before the disturbance the model disregards the forest disturbance
20 and its consequences on DIN and DOC production and leaching. It can therefore be used as a
21 base-line for the undisturbed system and as a tool for the quantification of additional nutrient
22 production. Our results indicate that the forest disturbance by windthrow results in a
23 significant increase of DIN production lasting ~3.7 years and exceeding the pre-disturbance
24 average by 2.7 kg/ha/a corresponding to an increase of 53%. There were no significant
25 changes of DOC concentrations. With simulated transit time distributions we show that the
26 impact on DIN travels through the hydrological system within some months. But a small
27 fraction of the system outflow (<5%) exceeds mean transit times of >1 year.

28 **1 Introduction**

29 Karst systems contribute around 50% to Austria's drinking water supply (COST, 1995). Karst
30 develops due to the dissolvability of carbonate rock (Ford and Williams, 2007) and it results
31 in strong heterogeneity of subsurface flow and storage characteristics (Bakalowicz, 2005).
32 The resulting complex hydrological behavior requires adapted field investigation techniques
33 (Goldscheider and Drew, 2007). Future climate trajectories indicate increasing temperature
34 (Christensen et al., 2007) and a higher frequency of hydrological extremes (Dai, 2012;
35 Hirabayashi et al., 2013). Both will influence the availability and quality of water provided
36 from karst regions because temperature triggers numerous biogeochemical processes and fast
37 throughflow water has a disproportional effect upon water quality. Also forest disturbances
38 (windthrows, insect infestations, droughts) pose a threat on water quality through the
39 mobilization of potential pollutants and these disturbances are likely to increase in future
40 (Johnson et al., 2010; Seidl et al., 2014).

41 A way to quantify the impact of changes in climatic boundary conditions on the hydrological
42 cycle are simulation models. Special model structures have to be applied for karst regions to
43 account for their particular hydrological behavior (Hartmann et al., 2014a). A range of models
44 of varying complexity is available from the literature, that deal with the karstic heterogeneity,
45 such as groundwater flow in the rock fracture matrix and dissolution conduits (Jourde et al.,
46 2015; Kordilla et al., 2012), varying recharge areas (Hartmann et al., 2013a; Le Moine et al.,
47 2008) or preferential recharge by cracks in the soil or fractured rock outcrops (Rimmer and
48 Salingar, 2006; Tritz et al., 2011).

49 Nitrate and dissolved organic carbon (DOC) have both been considered in drinking water
50 directives and water preparation processes (Gough et al., 2014; Mikkelsen et al., 2013; Tissier
51 et al., 2013; Weishaar et al., 2003). Though nitrate pollution of drinking water is usually
52 attributed to fertilization of crops and grassland, an excess input of atmospheric nitrogen (N)
53 from industry, traffic and agriculture into forests has caused reasonable nitrate losses from
54 forest areas (Butterbach-Bahl et al., 2011; Erisman and Vries, 2000; Gundersen et al., 2006;
55 Kiese et al., 2011). The Northern Limestone Alps area is exposed to particularly high nitrogen
56 deposition (Rogora et al., 2006) and nitrate leaching occurs in increased rates (Jost et al.,
57 2010). Apart from this, forest disturbances such as windthrow and insect outbreaks disrupt the
58 N cycle and cause pronounced nitrate losses from the soils, at least in N saturated systems,
59 that received elevated N deposition due to elevated NO_x in the atmosphere (Bernal et al.,

60 2012; Griffin et al., 2011; Huber, 2005). Contrary to N deposition, atmospheric deposition of
61 DOC is low (Lindroos et al., 2008) and thus has not been identified as major driver of DOC
62 leaching from subsoil (Fröberg et al., 2007; Kaiser and Kalbitz, 2012; Verstraeten et al.,
63 2014). Moreover, studies show contrasting results but point to increased DOC (TOC) leaching
64 from soil and catchments after forest disturbances (Huber et al., 2004; Löfgren et al., 2014;
65 Meyer et al., 1983; Mikkelsen et al., 2013; Wu et al., 2014).

66 While many studies identify N and DOC as source of contamination in karst systems
67 (Einsiedl et al., 2005; Jost et al., 2010; Katz et al., 2001, 2004; Tissier et al., 2013) or provide
68 static vulnerability maps (Andreo et al., 2008; Doerfliger et al., 1999), only very few studies
69 use models to quantify the temporal behavior of a contamination through the systems
70 (Butscher and Huggenberger, 2008). Some studies use N and DOC to better understand karst
71 processes (Charlier et al., 2012; Mahler and Garner, 2009; Pinault et al., 2001) or for
72 advanced karst model calibration (Hartmann et al., 2013b, 2014b) but from our knowledge
73 there are no applications of such approaches to quantify the drainage processes of N and
74 DOC, and particularly so after strong impacts on ecosystems (e.g. windthrow) that release
75 reasonable amount of nitrate from the forest soils.

76 In this study, we consider the time period before and after storm Kyrill (early 2007) and
77 several other storm events (2008) that hit Middle Europe. The storms, from now on referred
78 to as the wind disturbance period, caused strong damage to the forests in our study area, a
79 dolomite karst system. We apply a new type of semi-distributed model that considers the
80 spatial heterogeneity of the karst system by distribution functions. We aimed at comparing the
81 hydrological and hydrochemical behavior (DOC, DIN) of the system before and during the
82 wind disturbing period. In particular, we wanted to understand if and how DOC and DIN
83 input to the hydrological system changed by the impact of the storms. Furthermore, we used
84 virtual tracer experiments to create transit time distributions that expressed how the impact of
85 the storms propagated through the variable dynamic flow paths of the karst system. This
86 allowed us to assess the vulnerability of the karst catchment to such impacts.

87 **2 Study site**

88 The study site LTER Zöbelboden is located in the northern part of the national park
89 “Kalkalpen” (Figure 1). Its altitude ranges from 550 m to 956 m ASL and its area is ~5.7 km².
90 Mean monthly temperature varies from -1 °C in January to 15.5 °C in August. The average
91 temperature is 7.2 °C (at 900 m ASL). Annual precipitation ranges from 1,500 to 1,800 mm

92 and snow accumulates commonly between October and May with an average duration of
93 about 4 months. The mean N deposition in bulk precipitation between 1993 and 2006 was
94 18.7 kg N ha⁻¹.yr⁻¹, out of which 15.3 kg N (82%) was inorganic (approximately half as NO₃⁻-
95 N and half as NH₄⁺-N) (Jost et al., 2011). Due to the dominating dolomite, the catchment is
96 not as heavily karstified as limestone karst systems, but shows typical karst features such as
97 conduits and sink holes (Jost et al., 2010). The site can be split into steep slopes (30-70°, 550-
98 850 m ASL) and a plateau (850-950 m ASL), with the plateau covering ~0.6 km². Chromic
99 cambisols and hydromorphic stagnosols with an average thickness of 50 cm and lithic and
100 rendzic leptosols with an average thickness of 12 cm can be found at the plateau and the
101 slopes, respectively (WRB, 2006). Both plateau and slopes are mainly covered by forest.
102 Norway spruce (*Picea abies* L. Karst.) interspersed with beech (*Fagus sylvatica* L.) was
103 planted after a clear cut around the year 1910. The vegetation at the slopes is dominated by
104 semi-natural mixed mountain forest with beech (*Fagus sylvatica*) as the dominant species,
105 Norway spruce (*P. abies*), maple (*Acer pseudoplatanus*), and ash (*Fraxinus excelsior*). At the
106 slopes no forest management has been conducted since the implementation of the National
107 Park.

108 2.1 Available data

109 A 10 year record of input and output observations was available. Starting from the
110 hydrological year 2002/03 it envelops well the stormy period that began in January 2007. It
111 included daily rainfall measurements and stream discharge measurements from stream
112 sections 1 and 2 (Figure 1). We obtained the discharge of the entire system with a simple
113 topography based up-scaling procedure that is described in more detail in (Hartmann et al.,
114 2012a). Irregular (weekly to monthly) observations of DOC, DIN and SO₄²⁻ concentrations
115 are available for precipitation and at weir 1. DOC (~~entire study period~~), NO₃⁻, SO₄²⁻ and NH₄⁺
116 (since January 2010) samples were filtered (~~MILLIPOR HTP04700~~ (0.4 µm) before the
117 analysis. (~~Millipor Corporation, USA~~) with ~~SM 16249~~ (~~Sartorius AG, Germany~~) (~~xxxx-~~
118 ~~2009~~) and ~~SM 16201/19/20~~ (~~Sartorius AG, Germany~~) (~~2009-xxxx~~). NH₄⁺ concentrations were
119 measured after filtering by spectrophotometry (Milton Roy Spectronic) ~~1201~~ (~~Thermo Fisher~~
120 ~~Scientific Inc., USA~~). Weekly DOC, SO₄²⁻ and NO₃⁻ samples were pooled to provide volume
121 weighted bi-weekly (until March 2009) and monthly (thereafter) samples. DOC samples were
122 acidified with 0.5 ml HCl 25% and were measured with a Maihak Tocor 100 and a CPN
123 TOC/DOC-Analyzer (Shimadzu Corp., Japan). ~~All samples were kept at 4°C until analyses.~~

124 NO₃⁻ and SO₄²⁻ concentrations were determined by ion chromatography with conductivity
125 detection (~~Bulk precipitation: 2002-2009: Dionex ICS DX 500 (Dionex Corp., USA); 2010-~~
126 ~~xxxx: Dionex ICS 3000 (Dionex Corp., USA); Runoff: 2001-2002: Dionex ICS DX 500~~
127 ~~(Dionex Corp., USA); 2002-2010: Metrohm ICS 7xx (Deutsche METROHM GmbH & Co.~~
128 ~~KG, Germany)). DOC concentrations were measured with a Maihak Töcor 100 (SICK~~
129 ~~MAIHAK GmbH, Germany) (1996-2007) and a CPN TOC/DOC Analyzer (Shimadzu Corp.,~~
130 ~~Japan) (2007-2010). DIN input was then calculated as the sum of NO₃⁻-N and NH₄⁺-N. Since~~
131 NH₄⁺ is either transformed into NO₃⁻ or absorbed in the soil NH₄⁺ concentrations in runoff are
132 very small or not detectable. Therefore we calculated DIN outputs as NO₃⁻-N. Additionally,
133 irregular observations of snow water equivalent at the plateau allowed for independent setup
134 of the snow routines.

135 **2.2 Recent disturbances**

136 Kyrill in the year 2007 and some similarly strong storms that followed 2008 caused some
137 major windthrows as well as single tree damages. A windthrow disturbance of ~ 5 ha
138 occurred upstream of weir 1. Though no direct measurements exist as to the total extent of the
139 windthrow area we estimate that 5-10 % of the study site has been subject to windthrow
140 (Kobler et al., 2015). We did not observe a significant change in intra- and inter-annual
141 variability of DOC concentrations and discharge before and during the wind disturbance
142 period (Figure 2ae). Runoff concentrations of DIN showed clear responses to the
143 disturbances. With the first windthrow event it started to increase until 2008/09 and slowly
144 decreased again in 2010/11 (Figure 2c). Comparing DOC concentrations with discharge
145 before and during the wind disturbance period revealed a similar pattern. As shown by other
146 studies on DOC mobilization (e.g., Raymond and Saiers, 2010), a positive correlation
147 between concentrations and discharge (on log₁₀ scale) occurred for DOC with concentrations
148 up to 6 mg/l during high discharge (similar to Frank et al., 2000). But there was no obvious
149 difference between the pre-disturbance period (Figure 2b).

150 3 Methods

151 3.1 The model

152 3.1.1 Model hydrodynamics

153 The semi-distributed simulation model considers the variability of karst system properties by
154 statistical distribution functions spread over $Z=15$ model compartments (Figure 3). That way
155 it simulates a range of variably dynamic pathways through the karst system. The detailed
156 equations of the model hydrodynamics are similar to its previous applications (Hartmann et
157 al., 2013a, 2013c, 2014b). They are described in the Appendix. Since in our case the model is
158 used to simulate the discharge of the entire system and a weir within the system some small
159 modifications had to be performed. Preceding studies showed that weir 1 (Figure 1) receives
160 its discharge partially from the epikarst and partially from the groundwater, reaching it
161 partially as concentrated and partially as diffuse flow (Hartmann et al., 2012a). Consequently
162 we derive its discharge Q_{weir} [l/s] by

$$163 \quad Q_{weir}(t) = f_{Epi} \cdot \left[f_{Epi,conc} \cdot \sum_i^Z R_{conc,i}(t) + (1 - f_{Epi,conc}) \cdot \sum_i^Z R_{diff,i}(t) \right] + \\ \left(1 - f_{Epi} \right) \cdot \left[f_{GW,conc} \cdot Q_{GW,Z}(t) + (1 - f_{GW,conc}) \cdot \sum_i^{Z-1} Q_{GW,i}(t) \right] \quad (1)$$

164 Where f_{Epi} is the fraction from the epikarst and $(1-f_{Epi})$ the fraction from the groundwater.
165 $f_{Epi,conc}$ and $f_{GW,conc}$ represent the concentrated flow fractions of the epikarst and groundwater
166 contributions, respectively. Table 1 lists all model parameters including a short description.

167 3.1.2 Model solute transport

168 To model the non-conservative transport of DOC and, DIN and SO_4^{2-} , we equipped the model
169 with solute transport routines. SO_4^{2-} was included as an additional calibration variable
170 because it proved to be important to reduce model equifinality (Beven, 2006) by adding
171 additional information about groundwater dynamics (Hartmann et al., 2013a, 2013b). The
172 inclusion of these 3 solutes allowed for a more reliable estimation of model parameters
173 (Hartmann et al., 2012b, 2013a) and, further on, the evaluation of possible changes in the
174 dynamic of solute concentrations during the stormy period. For most of the model
175 compartments they simply followed the assumption of complete mixing. But to represent net
176 production and leaching of DOC and DIN in the soil, as well as dissolution of SO_4^{2-} in the

177 rock matrix, additional processes were included in the model structure. Similar to preceding
 178 studies (Hartmann et al., 2013a, 2014b) SO_4^{2-} dissolution $G_{\text{SO}_4,i}$ [mg/l] for compartment i is
 179 calculated by:

$$180 \quad G_{\text{SO}_4,i} = G_{\text{max,SO}_4} \cdot \left(\frac{Z-i+1}{Z} \right)^{a_{\text{Geo}}} \quad (2)$$

181 where a_{Geo} [-] is another variability parameter and $G_{\text{max,SO}_4}$ [mg/l] is the equilibrium
 182 concentration of SO_4^{2-} in the matrix. DOC is mostly mobilised at in the forest floor (Borken et
 183 al., 2011). Stored in the soil or diffusively and slowly passing downwards, large parts of the
 184 DOC is absorbed or consumed by micro-organisms. But when lateral flow and concentrated
 185 infiltration increase net leaching of DOC increases as well. For that reason our DOC transport
 186 routine only provides water to the epikarst when it is saturated (Eq. 10) with increasing DOC
 187 net production toward the more dynamic model compartments (Figure 3). Its DOC
 188 concentration $P_{\text{DOC},i}$ [mg/l] for each model compartment is found by:

$$189 \quad P_{\text{DOC},i} = P_{\text{DOC}} \cdot \left(\frac{Z-i+1}{Z} \right)^{\frac{1}{a_{\text{DOC}}}} \quad (3)$$

190 where a_{DOC} [-] is the DOC variability constant and P_{DOC} [mg/l] is the DOC net production at
 191 soil compartment 1. Similar to other studies that assessed N input to a karst system (Pinault et
 192 al., 2001) we used a trigonometric series to assess the time variant net production of DIN,
 193 $P_{\text{DIN},i}$ [mg/l], to the soil:

$$194 \quad P_{\text{DIN},i} = P_{\text{DIN}} + A_{\text{DIN}} \cdot \sin\left(\frac{365.25}{2\pi} \cdot (J_D + S_{\text{PH,DIN}}) \right) \quad (4)$$

195 Here, P_{DIN} is the mean amount of dissolved inorganic N in the soil solution, while A_N [mg/l]
 196 and $S_{\text{PH,DIN}}$ [d] are the amplitude of the seasonal signal and the phase shift of seasonal DIN
 197 uptake (immobilisation by plants and soil organisms) and release (net DIN in the soil water)
 198 cycle, respectively. J_D is the Julian day of each calendar year. Due to its seasonal variation
 199 $P_{\text{DIN},i}$ can also be negative meaning that uptake of DIN takes place.

200 3.2 Model calibration and evaluation

201 With 14 model parameter that controlled the hydrodynamics and 7 parameters that allow for
 202 the non-conservative solute transport, the calibration of the model was a high-dimensional
 203 problem. For that reason we have chosen the Shuffled Complex Evolution Metropolis

204 algorithm SCEM (Vrugt et al., 2003) that prove itself to be capable of exploring high
205 dimensional optimization problems (Fenicia et al., 2014; Feyen et al., 2007; Vrugt et al.,
206 2006). As performance measure we used the Kling-Gupta efficiency KGE (Gupta et al.,
207 2009). For calibration, KGE was weighted equally among all solutes, 1/3 for the discharge of
208 the entire system, and 2/3 for the discharge of weir 1 whose observations precision was
209 regarded to be more reliable than the up-scaled discharge. KGE is defined as:

$$210 \quad KGE = 1 - \sqrt{(r-1)^2 + (\alpha-1)^2 + (\beta-1)^2} \quad (5)$$

$$211 \quad \text{with } \alpha = \frac{\sigma_s}{\sigma_o} \text{ and } \beta = \frac{\mu_s}{\mu_o} \quad (6)$$

212 where r is the linear correlation coefficient between simulations and observations, μ_s/μ_o and
213 σ_s/σ_o are the means and standard deviations of simulations and observations, respectively. α
214 expresses the variability and β the bias.

215 To check for the stability of the calibrated parameters, we perform a split-sample test
216 (Klemeš, 1986). Since the pre-disturbance time series was too short to be split into two
217 equally long periods, we perform a both-sided split-sample test by bootstrapping two
218 independent 4-year time series of observations (1st sample: discrete sampling of 50% of the
219 values of each observed time series, 2nd sample: remaining 50% of the observations). We
220 calibrate our model with the 1st sample and evaluate it with the 2nd sample, and vice versa. A
221 parameter set is regarded stable, when the calibration with both samples yields similar
222 parameter sets and their KGE concerning discharge and the solutes does not reduce
223 significantly when applying them on the other sample.

224 3.3 Change of hydrochemical behaviour with the stormy period

225 After the model evaluation, we use the different components of the KGE in Eqs. (5) and (6) to
226 explore the impacts of the storm disturbance period on the hydrochemical components.
227 Assuming that the model is able to predict to hydrochemical behaviour that prevailed without
228 the impact of the storms adapting the hydrochemical parameters of the model in Eqs. (3)-(4)
229 and analysing the difference between the adapted hydrochemical simulations and the non-
230 adapted simulations will allow us to quantify the change of solute mass balance due to the
231 storm impact. We define the time span for our adaption as the time when the different
232 components of KGE exceed the range of their pre-disturbance variability. During this time

233 period we compensate for the apparent deviations by adapting the hydrochemical parameters.
234 This is done twice, once by manual adaption and another time using an automatic calibration
235 scheme. Their new values will indicate changes of the seasonality, production or inter-annual
236 variations.

237 **3.4 Transit time distributions**

238 The signal of the storm impact will travel by various velocities and pathways through the
239 karst system. While fast flow paths and small storages will transport the signal rapidly to the
240 system outlet, slow pathways and large storages will delay and dilute the signal. Transit time
241 distributions indicate how fast surface impacts travel through the hydrological system. We
242 derive transit time distributions from the model by performing a virtual tracer experiment
243 with continuous injection over the entire catchment at the beginning of the impact of the
244 stormy period. When a model compartment reaches 50% of the tracer concentration is
245 considered as median transit time. The hereby-derived transit times will elaborate how the
246 hydrological system propagates the signal through the system including all slow and fast
247 pathways as defined by Eqs. (12) and (18). As for DIN and DOC we assume complete and
248 instantaneous mixing with each model storage (soil, epikarst, and groundwater) at each
249 compartment, the time that we refer to as “mean transit time” of a model compartment is the
250 time the virtual tracer needs to pass through the particular model storage. In combination with
251 the fluxes that are provided from each of the model compartments, it is possible to quantify
252 the fractional contribution of fast and slow flow paths, respectively. We will apply the virtual
253 tracer from the previously assessed beginning of the impact until the end of the time series to
254 assess the transit time distribution. In addition, we apply a second virtual tracer that also lasts
255 only for the disturbance period (as estimated in subsection 3.3) to evaluate the filter and
256 retardation potential of the karst system.

257 **4 Results**

258 **4.1 Model performance**

259 Table 1 shows the calibrated parameters for the two samples. They indicate a thick soil and a
260 relatively thin epikarst. The dynamics expressed by the storage constants indicate days and
261 weeks for the conduits (model compartment $i=Z$) and the epikarst, respectively. The
262 distribution coefficient of the groundwater is larger than the soil/epikarst storage constant. For

263 DOC and DIN there are a natural production rates of 1.6-1.8 mg/l and -1.35-0.1 mg/l,
264 respectively. The DOC distribution coefficient is between 0.9 and 1.1. The phase shift and
265 amplitude for DIN showed that there is a seasonal variation of DIN net production with its
266 maximum release at April each year for both of the samples. SO_4^{2-} is dominated by the
267 concentration in the precipitation input with some leaching in the soil and sulphides in the
268 dolomite. Its variability constant is quite low (<0.1). Weighted KGEs, as well as their values
269 for the individual simulation variables are relatively stable. Overall, calibration on both
270 samples provided similar parameter values. Due to its higher stability concerning the
271 evaluation period, we chose the 2nd sample for further analysis.

272 The discharge simulations follow adequately the variations of the observations (Figure 4),
273 although some small events are not reproduced by the model and although the simulations of
274 the weir's discharge tend to under-estimate peak flows. No obvious differences can be seen
275 between the pre-disturbance and wind disturbance period. The hydrochemical simulations
276 tend to follow the observations, as well (Figure 5). But there is sometimes some under-
277 estimation of the DOC peaks for the pre-disturbance period. The DIN simulations appear to
278 be more precise during the pre-disturbance period but there is a systematic under-estimation
279 when the disturbance takes place.

280 **4.2 Model performance during the wind disturbance period**

281 There is a deviation between pre-disturbance and disturbance period simulated and observed
282 variability and bias for DIN (Figure 6). A similar tendency can be found for DOC. But only
283 for DIN the deviations are different to the variations already found during the pre-disturbance
284 period (which is also the calibration/validation period). The variations of DOC appear to be
285 systematic, too, but they fall within its ranges of variability during the pre-disturbance period.

286 **4.3 Adaption of N parameters for the wind disturbance period**

287 The very first signs of the impact were found at May 1st 2007 lasting to the end of the
288 hydrological year 2010/11. In a first trial (Table 2), the model parameters for the DIN
289 production were adapted manually to compensate for the changes of observed DIN
290 concentrations with focus on reducing the difference indicated by the bias β and variability α
291 components of the KGE_{DIN} . In a second trial, we use an automatic calibration scheme to
292 achieve the optimum KGE_{DIN} . As indicated by the highest KGE (Table 2), the automatic

293 calibration provided the highest KGE_{DIN} . But this is achieved by improving variability α and
294 correlation r . Almost no improvement is reached for the bias β . Even though resulting in a
295 slightly lower improvement of KGE_{DIN} the manual calibration results in a much more
296 acceptable reduction of the bias (Figure 6). Its parameter values showed a production rate
297 P_{DIN} of DIN ~~more than almost two times~~ 2 mg/l larger than the pre-disturbance value, an
298 amplitude A_{DIN} ~~more around than 41 times mg/l larger~~ smaller, and a phase shift $S_{PH,DIN}$
299 towards a week earlier in the year, resulting in a more acceptable simulation of DIN dynamics
300 during the disturbance period (Figure 7).

301 4.4 Transit time distributions

302 The transit time distributions show that the soil and epikarst system reacts quite rapidly to the
303 virtual injection. 50% of the injection concentration is reached within ~60 days (Figure 8a),
304 while most of groundwater system requires ~100 days to reach 50% of the injection
305 concentration with few flow paths reach up to 300 days (Figure 8c). A similar behaviour is
306 found when the impact ends (Figure 8bd). It also shows that some of the slowest flow paths
307 just reach the input concentration before they start to decline again.

308 5 Discussion

309 5.1 Reliability of calibrated parameters and model simulations

310 Most of the calibrated model parameters are in ranges that are in accordance with other
311 modelling studies or field evidence. General differences between the calibrated parameter
312 values of the both-sided split sample test may mostly be due to the comparatively low
313 resolution of the hydrochemical variables (SO_4 , DOC and DIN) that even increased by the
314 bootstrapping procedure. However, the good multi-objective simulation performance of the
315 model, as well as its evaluation by the split sample test an overall acceptable performance of
316 the model. With almost 3-8 days the epikarst storage constant is in accordance with field
317 studies on the epikarst storage behaviour that found retention times of some days to few
318 weeks (Aquilina et al., 2006; Perrin et al., 2003). The soil as well as the epikarst storage
319 capacity are quite large. These high values may be explained by structural errors of the model
320 that result in unrealistic calibrated parameter values, in particular possible parameter
321 interactions between their storage capacities and storage coefficients. Since the soil and the
322 vegetation controls the fraction of rain that is lost to evapotranspiration this high calibrated

Formatiert: Englisch (Großbritannien)

323 value might be due to tree roots ranging through the soil into the epikarst (Heilman et al.,
324 2012) or rock debris (Hartmann et al., 2012a).

325 Similar to the epikarst storage constant, the conduit storage constant, K_C , is, with its value of
326 1.1 days, in the range of previous modelling studies (Fleury et al., 2007; Hartmann et al.,
327 2013a). The high values of the epikarst variability constant and the groundwater constant
328 indicate a low development of preferential flow paths in the rock, which is typical for
329 dolomite aquifers (Ford and Williams, 2007). A low degree of karstification was already
330 known for our study site (Jost et al., 2010) and the calibrated recharge areas fall well into the
331 ranges found in previous modelling studies (Hartmann et al., 2012a, 2013c).

332 The hydrochemical parameters mostly show realistic values. A DOC production parameter
333 P_{DOC} of ~1.6-1.8 mg/l resulted in realistic simulated concentrations at the weir. For DIN
334 production the two calibration samples result in values of -1.4 and 0.1 mg/l, going along with
335 amplitudes of 3.4 and 1.8, respectively. Hence, there appears to be some correlation between
336 the production and amplitude parameters, P_{DIN} and A_{DIN} . Negative values indicate that during
337 some periods of the year all DIN is consumed by plants or soil organisms and that the
338 production period is shorter, but more pronounced due to its larger value of amplitude. But we
339 expect these differences to be minor since the phase shift $S_{PH,DIN}$ of both calibration samples is
340 almost the same, as well as their annual maximum ($P_{DIN} + A_{DIN}$) of 2.01 mg/l and 1.95 mg/l. It
341 indicates a maximum of DIN production and leaching at the time of the year when snow melt
342 reaches its maximum (March to April) and when DIN uptake by plants is still low (Jost et al.,
343 2010). The dissolution equilibrium concentrations of 2.7-3.1 mg/l for SO_4^{2-} indicate the
344 abundance of the precipitation-input, oxidation of sulphides (e.g. pyrite) in the dolomite and
345 traces of evaporates in the small Plattenkalk occurrences (Kralik et al., 2006).

346 **5.2 Impact of storms**

347 The deviation between simulated and observed time series (Figure 5) already indicates that
348 DIN is the only solute that shows a clear impact of the storms. This is further corroborated by
349 considering the individual components of KGE in Figure 6. It is well known that nitrate
350 leaching to the groundwater increases sharply after tree damage (dieback) in forests where N
351 is not strongly limited (Bernal et al., 2012; Griffin et al., 2011; Huber, 2005). Such
352 disturbances disrupt the N cycle. The loss of tree N uptake favours nitrification of surplus
353 NH_4^+ by microorganism. Moreover, above- (i.e. foliage) and belowground (i.e. fine roots)

354 litter from dead trees enhances the mineralization of organic matter, ammonification and
355 nitrification. Both processes are accelerated by increased soil moisture and soil temperature
356 due to the loss of the forest canopy. Subsequently, leaching of N increases with increased
357 seepage fluxes due to decreased interception and water uptake by trees. Since the simple DIN
358 routine of the model cannot take into account such changes the under-estimated DIN
359 concentrations and their amplitude show the effect of forest disturbance on the leaching of
360 DIN from the studied catchment. There is also an apparently systematic deviation of the DOC
361 variability α . But its variations during the pre-storm period are similarly large and thus points
362 to a negligible effect of forest disturbance on DOC leaching. Numerous studies identified the
363 forest floor as DOC source (Borken et al., 2011; Michalzik et al., 2001). Windthrow generally
364 causes a (short-term) pulse of above- and belowground litter (Harmon et al., 2011). Thereby,
365 mineralization of the surplus litter input concurrent with improved soil climatic conditions
366 likely increased the leaching of DOC from the forest floor (Fröberg et al., 2007; Kalbitz et al.,
367 2007). Concurrent, increased soil water, surface and shallow subsurface flow may favour
368 increased soil DOC leaching to downslope surface waters (Monteith et al., 2006; Neff and
369 Asner, 2001; Sanderman et al., 2009). In mountainous catchment the latter flow paths are
370 likely due to the steepness of the catchment slopes (Boyer et al., 1997; Sakamoto et al., 1999;
371 Terajima and Moriizumi, 2013). The missing signal of forest disturbance on DOC
372 concentrations at the weir 1 even shortly after the disturbance may be due to the minor
373 extension of the disturbed area, the minor increase of surface and shallow subsurface flow due
374 to the relative low slope of the disturbed area, the buffering of increased topsoil DOC
375 leaching due to absorption of DOC within the subsoil (Borken et al., 2011; Huber et al.,
376 2004), missing DOC-rich riparian source areas (i.e. wetlands, floodplains) and the reduction
377 pre-disturbance organic matter input to soil (i.e. litter, root exudates) (Högberg and Högberg,
378 2002). Theoretically, hydrological processes such as a decrease of transpiration or an increase
379 of groundwater recharge may also occur. But these superficial changes are probably minor
380 considering the typically high karstic infiltration capacities that remove surface water quite
381 rapidly (Hartmann et al., 2014b, 2015). Therefore, hydrological impacts of windthrow on
382 karst systems (for instance on transpiration) may not be as pronounced as in non-karstic
383 domains because a large fraction of the infiltration during high flow periods will not be
384 available for transpiration anyway. Consequently, a disturbance caused impact on DOC
385 availability could also be hidden because increased infiltration and DOC leaching during
386 strong rainfall events may just not be detectable considering the weekly to monthly sampling

387 of DOC. For both a better understanding of, disturbance induced changes of DOC ~~and~~
388 ~~hydrological processes,~~ more sampling in high temporal-resolution of DOC and DIN
389 concentrations at the weir (Figure 1) should be undertaken to elucidate the effect of forest
390 disturbance on DOC dynamics and to improve the simulation of DOC production and
391 transport within the studied ecosystem to elucidate the effect of forest disturbance within the
392 studied ecosystem.

393 **5.2.1 N leaching from the soil**

394 Adapting the DIN solute transport parameters by an automatic calibration scheme resulted in
395 an increased KGE_{DIN} (Figure 7). But it did not resolve the bias of simulated and observed DIN
396 concentrations during the wind disturbance period since the overall improvement of KGE_{DIN}
397 was reached by an improvement of r and α (Table 2). Adjusting the DIN parameters manually
398 resulted in a more acceptable decrease of the bias β that also went along with an increase of
399 the overall KGE_{DIN} . An increase of the DIN production rate of ~ 2 mg/l indicates a massive
400 mobilisation of DIN and a reduction of its seasonal amplitude by ~ 1.1 mg/l. Even though
401 there may be some correlation between mean annual production and amplitude (see previous
402 section), the annual maximum of 2.80 mg/l ($P_{DIN} + A_{DIN}$) indicates an increase of the DIN
403 concentrations in the soil of at least ~ 0.8 mg/l (from 1.95 to 2.01 mg/l at the pre-disturbance
404 period).

405 We identified the beginning of the impact at May 1st 2007 and its end by the end of the
406 hydrological year 2010/11. This is more than 2 years after the last storm in 2008 indicates
407 how long the ecosystem takes to recover from the disturbance. Other studies have shown
408 comparable recovery times (Katzensteiner, 2003; Weis et al., 2006) or longer (Huber, 2005).
409 Considering the deviations between DIN simulations by the pre-disturbance calibration and
410 the DIN simulations obtained by the manual adjustment, they sum up to an additional release
411 of 9.9 kg/ha of DIN over the whole period of ~ 3.7 years, or 2.7 kg/ha/a in addition to 5.8
412 kg/ha/a that would have been released without the wind disturbance. These values only
413 corresponds to inorganic N. Other studies showed that also dissolved organic N can contribute
414 to vertical percolation but only in small ratios from 2-5% (Solinger et al., 2001; Wu et al.,
415 2009). The apparent shift of $S_{PH,DIN}$ towards an earlier maximum of DIN release (7 days) may
416 is most probably be due to the earlier onset of snow melt in open areas as compared to forests
417 because snow melt is a major driver of- DIN leaching from the soils in our study area (Jost et
418 al., 2010). However, due to the rather slow melting rates, most of the melting water will

419 slowly/diffusively enter the groundwater system rather than flowing rapidly through the karst
420 conduits. Therefore, a slightly earlier beginning of snowmelt may not be visible at the system
421 outlet due to the slow reaction of the groundwater storage.

422 **5.2.2 N propagation through the hydrological system**

423 The virtual tracer injections that we applied with the beginning of the disturbance period
424 elaborate the hydrological system's filter and retardation capacity. Due to their higher
425 dynamics the soil and the epikarst system adapt more rapidly to the change within weeks and
426 months. Similar behaviour was also found in previous studies (Hartmann et al., 2012a; Kralik
427 et al., 2009). The majority of the simulated flow paths adapts to the virtual tracer signal within
428 a few months, which is in accordance with water isotope studies as the weir (Humer and
429 Kralik, 2008; Kralik et al., 2009). However, using age dating (CFC and SF6) and artificial
430 tracer experiments at individual springs within the study area, the Kralik et al. (2009) also
431 found ages from several days to several decades. Hence, the majority of transit times found by
432 the virtual tracer experiment reflect the average behaviour of the sub-catchment drained by
433 the weir, which can be regarded as more dominant than observations at individual the springs
434 that rather represent fast and slow flow paths of minor importance. The retardation is also
435 visible from the dynamics of the DIN concentrations just after the end of the disturbance
436 period (beginning of 2011/12, Figure 7). Even though DIN production is set to pre-
437 disturbance conditions, it almost takes 4 months for the DIN simulations (by manual
438 calibration) to adopt to their undisturbed concentrations (pre-disturbance calibration). Due to
439 their small contribution (<5%), the slower flow paths do not have a significant impact on the
440 retardation capacity of the hydrological system.

441 **5.3 Implications**

442 Our results corroborate findings from many other studies that extreme events as during the
443 wind disturbance period in our study can result in significant increase of DIN in the runoff,
444 despite the area impacted was relative small (5-10% of the watershed). Particularly in karst
445 catchments such changes can happen quickly and prevail for a significant duration, in our
446 case more than 2 years after the last storm. Due to subsurface heterogeneity the impact did not
447 travel uniformly through the system. It rather split into different pathways and mixed with old
448 water that percolated prior to the impact. In our system, large parts of the water travelled
449 rapidly through the system. But a smaller number of pathways had large storages of old water

450 and slow flow velocities resulting in significant retardation. Taking into account that forest
451 disturbances will most probably increase with climate change (Seidl et al., 2014), DIN
452 mobilisation as observed in our study may occur more often and more intense. The
453 hydrological system may dilute and delay rapid shifts of N concentration, and it will
454 “memorize” the impacts for some time. But our present analysis showed that the time scale of
455 the wind disturbance on DIN production and leaching from the soil exceeds the time scale of
456 transit of the disturbance through the system. This is most probably due to the small size and
457 the subsurface karstic behaviour of our study site that favours faster flow paths and low
458 system storage than hydrological systems with larger extent or with other types of geology.

459 **6 Conclusions**

460 In our study we used a process-based semi distributed karst model to simulate DOC, DIN and
461 SO_4^{2-} transport through a dolomite karst system in Austria. We calibrated and validated our
462 model during a 4-year time period just before a series of heavy storms caused strong wind
463 disturbance to the study site’ ecosystem. To quantify its impact we run the model for the
464 entire disturbance period using the parameters we found at the pre-storm period. The
465 deviations between the simulations and the observations gave us indication that there was a
466 significant shift in DIN mobilisation, its seasonal amplitude and its timing. Estimating the
467 beginning and end of the disturbance period we applied a continuous virtual tracer injection to
468 obtain the mean transit times of the karst system. They showed us how the hydrological
469 system filtered and retarded the impact of the disturbance at the system outlet.

470 Even though our study is only considering one site and one wind disturbance period it already
471 provides some generally applicable conclusions: (1) hydroclimatic extremes such as storms
472 do not only create droughts or floods; they can also affect water quality; (2) a hydrological
473 system can filter and delay surface impacts but it may also memorize past impacts but only at
474 a limited time scale; (3) water quality models that have been calibrated without consideration
475 of such external impacts will provide poor predictions. For these reasons we believe that
476 future large-scale simulations of water resources have to include water quality simulations
477 that take into account the impact of ecosystem disturbances. Even without anthropogenic
478 contamination climate change will strongly affect water quality in our aquifers and streams
479 and we have to understand and prepare ourselves to avoid threats on future water supply.

480 7 Acknowledgements

481 Financial support by the Transnational Access to Research Infrastructures activity in the 7th
482 Framework Programme of the EC under the ExpeER project and the South East Europe
483 Transnational Cooperation Programme OrientGate for conducting the research is gratefully
484 acknowledged. This work was supported by a fellowship within the Postdoc Programme of
485 the German Academic Exchange Service (DAAD).

486 8 Appendix

487 The variability of soil depths in the model is expressed by a mean soil depth $V_{mean,S}$ [mm] and
488 a distribution coefficient a_{SE} [-]. The soil storage capacity $V_{S,i}$ [mm] for every compartment i
489 is calculated by:

$$490 \quad V_{S,i} = (1 - f_{var,S}) \cdot V_{mean,S} + V_{max,S} \cdot \left(\frac{i}{Z}\right)^{a_{SE}} \quad (7)$$

491 Where the maximum soil storage capacity $V_{max,S}$ [mm] is derived from $(f_{var,S} \cdot V_{mean,S})$ as
492 described in Hartmann et al. (2013c). $f_{var,S}$ [-] is the fraction of the soil that shows variable
493 thicknesses while $(1 - f_{var,S})$ has uniform value. The same distribution coefficient a_{SE} is used to
494 define the epikarst storage distribution by the mean epikarst depth $V_{mean,E}$ [mm] (derivation of
495 $V_{max,E}$ identical to $V_{mean,S}$):

$$496 \quad V_{E,i} = V_{max,E} \cdot \left(\frac{i}{Z}\right)^{a_{SE}} \quad (8)$$

497 Actual evapotranspiration from each soil compartment at time step t $E_{act,i}$ is found by:

$$498 \quad E_{act,i}(t) = E_{pot}(t) \cdot \frac{\min[V_{Soil,i}(t) + P(t) + Q_{Surface,i}(t), V_{S,i}]}{V_{S,i}} \quad (9)$$

499 where $Q_{Surface,i}$ [mm/d] is the surface inflow originating from compartment $i-1$ (see Eq. (13)),
500 E_{pot} [mm/d] the potential evaporation, and P [mm/d] the precipitation at time t . E_{pot} is
501 calculated by the Penman-Wendling approach (Wendling et al., 1991; DVWK, 1996). To
502 account for the solid fraction of precipitation a snowmelt routine was set on top of the model.
503 We used the same routine that was applied on 148 other catchments in Austria by Parajka et
504 al. (2007) and explained in Hartmann et al. (2012). Recharge to the epikarst $R_{Epi,i}$ [mm/d] is
505 defined as:

506
$$R_{Epi,i}(t) = \max[V_{Soil,i}(t) + P(t) + Q_{Surface,i}(t) - E_{act,i}(t) - V_{S,i}, 0]$$
 (10)

507 Where the storage coefficients $K_{E,i}$ [d] control the outflow of the epikarst:

508
$$Q_{Epi,i}(t) = \frac{\min[V_{Epi,i}(t) + R_{Epi,i}(t) + Q_{Surface,i}(t), V_{E,i}]}{K_{E,i}} \cdot \Delta t$$
 (11)

509
$$K_{E,i} = K_{max,E} \cdot \left(\frac{Z-i+1}{Z}\right)^{a_{SE}}$$
 (12)

510 $K_{max,E}$ is derived by a mean epikarst storage coefficient $K_{mean,E}$ (see Hartmann et al., 2013c).

511 Excess water from the soil and epikarst that produces surface flow to the next model

512 compartment $Q_{Surf,i+1}$ [mm/d] is calculated by:

513
$$Q_{Surf,i+1}(t) = \max[V_{Epi,i}(t) + R_{Epi,i}(t) - V_{E,i}, 0]$$
 (13)

514 The lower outflow of each epikarst compartment is separated into diffuse ($R_{diff,i}$ [mm/d]) and

515 concentrated groundwater recharge ($R_{conc,i}$ [mm/d]) by the recharge separation factor $f_{C,i}$ [-]:

516
$$R_{conc,i}(t) = f_{C,i} \cdot Q_{Epi,i}(t)$$
 (14)

517
$$R_{diff,i}(t) = (1 - f_{C,i}) \cdot Q_{Epi,i}(t)$$
 (15)

518 The distribution of $f_{C,i}$ among the different compartments is defined by the distribution

519 coefficient a_{sep} :

520
$$f_{C,i} = \left(\frac{i}{Z}\right)^{a_{sep}}$$
 (16)

521 Diffuse recharge reaches the groundwater compartment below, while concentrated recharge is

522 routed to the conduit system (compartment $i = Z$). The variable contributions of the

523 groundwater compartments that represent diffuse flow through the matrix ($1 \dots Z - 1$) are

524 given by

525
$$Q_{GW,i}(t) = \frac{V_{GW,i}(t) + R_{diff,i}(t)}{K_{GW,i}}$$
 (17)

526 $K_{GW,i}$ is calculated by:

527
$$K_{GW,i} = K_C \cdot \left(\frac{Z-i+1}{Z}\right)^{-a_{GW}}$$
 (18)

528 where K_C is the conduit storage coefficient. The groundwater contribution of the conduit
529 system originates from compartment Z:

$$530 \quad Q_{GW,Z}(t) = \frac{\min \left[V_{GW,Z}(t) + \sum_{i=1}^Z R_{concd,i}(t), V_{crit,OF} \right]}{K_C} \quad (19)$$

531 Knowing the recharge area A_{max} [km²] and rescaling the dimensions [l s⁻¹], the discharge of
532 the entire system Q [l s⁻¹] is calculated by:

$$533 \quad Q(t) = \frac{A_{max}}{Z} \cdot \sum_{i=1}^Z Q_{GW,i}(t) \quad (20)$$

534

535 9 References

- 536 Andreo, B., Ravbar, N. and Vías, J. M.: Source vulnerability mapping in carbonate (karst)
537 aquifers by extension of the COP method: application to pilot sites, *Hydrogeol. J.*, 17(3), 749–
538 758, doi:10.1007/s10040-008-0391-1, 2008.
- 539 Aquilina, L., Ladouche, B. and Doerfliger, N.: Water storage and transfer in the epikarst of
540 karstic systems during high flow periods, *J. Hydrol.*, 327, 472–485, 2006.
- 541 Bakalowicz, M.: Karst groundwater: a challenge for new resources, *Hydrogeol. J.*, 13, 148–
542 160, 2005.
- 543 Bernal, S., Hedin, L. O., Likens, G. E., Gerber, S. and Buso, D. C.: Complex response of the
544 forest nitrogen cycle to climate change, , doi:10.1073/pnas.1121448109/-
545 /DCSupplemental.www.pnas.org/cgi/doi/10.1073/pnas.1121448109, 2012.
- 546 Beven, K. J.: A manifesto for the equifinality thesis, *J. Hydrol.*, 320(1-2), 18–36 [online]
547 Available from: [http://www.sciencedirect.com/science/article/B6V6C-4H16S4M-](http://www.sciencedirect.com/science/article/B6V6C-4H16S4M-1/2/571c8821621c803522cc823147bef169)
548 [1/2/571c8821621c803522cc823147bef169](http://www.sciencedirect.com/science/article/B6V6C-4H16S4M-1/2/571c8821621c803522cc823147bef169), 2006.
- 549 Borken, W., Ahrens, B., Schulz, C. and Zimmermann, L.: Site-to-site variability and temporal
550 trends of DOC concentrations and fluxes in temperate forest soils, *Glob. Chang. Biol.*, 17(7),
551 2428–2443, doi:10.1111/j.1365-2486.2011.02390.x, 2011.
- 552 Boyer, E. W., Hornberger, G. M., Bencala, K. E. and McKnight, D. M.: Response
553 characteristics of DOC flushing in an alpine catchment, *Hydrol. Process.*, 11(12), 1635–1647,
554 doi:10.1002/(SICI)1099-1085(19971015)11:12<1635::AID-HYP494>3.0.CO;2-H, 1997.
- 555 Butscher, C. and Huggenberger, P.: Intrinsic vulnerability assessment in karst areas: A
556 numerical modeling approach, *Water Resour. Res.*, 44, W03408,
557 doi:10.1029/2007WR006277, 2008.

558 Butterbach-Bahl, K., Gundersen, P., Ambus, P., Augustin, J., Beier, C., Boeckx, P.,
559 Dannenmann, M., Sanchez Gimeno, B., Ibrom, A. and Kiese, R.: Nitrogen processes in
560 terrestrial ecosystems, *Eur. nitrogen Assess. sources, Eff. policy Perspect.*, 99–125, 2011.

561 Charlier, J.-B., Bertrand, C. and Mudry, J.: Conceptual hydrogeological model of flow and
562 transport of dissolved organic carbon in a small Jura karst system, *J. Hydrol.*, 460-461, 52–64,
563 doi:10.1016/j.jhydrol.2012.06.043, 2012.

564 Christensen, J. H., Hewitson, B., Busuioic, A., Chen, A., Gao, X., Held, I., Jones, R., Kolli, R.
565 K., Kwon, W.-T., Laprise, R., Rueda, V. M., Mearns, L., Menéndez, C. G., Räisänen, J.,
566 Rinke, A., Sarr, A. and Whetton, P.: Regional Climate Projections, in *Climate Change 2007:
567 The Physical Science Basis. Contribution of Working Group I to the Fourth Assessment
568 Report of the Intergovernmental Panel on Climate Change*, edited by S. Solomon, D. Qin, M.
569 Manning, Z. Chen, M. Marquis, K. B. Averyt, M. Tignor, and H. L. Miller, p. 996,
570 Cambridge University Press, Cambridge, United Kingdom and New York, NY, USA. [online]
571 Available from:
572 [http://www.ipcc.ch/publications_and_data/publications_ipcc_fourth_assessment_report_wg1_](http://www.ipcc.ch/publications_and_data/publications_ipcc_fourth_assessment_report_wg1_report_the_physical_science_basis.htm)
573 [report_the_physical_science_basis.htm](http://www.ipcc.ch/publications_and_data/publications_ipcc_fourth_assessment_report_wg1_report_the_physical_science_basis.htm), 2007.

574 COST: COST 65: Hydrogeological aspects of groundwater protection in karstic areas, Final
575 report (COST action 65), edited by D.-G. X. I. I. S. European Commission Research and
576 Development, *Eur. Comm. Dir. XII Sci. Res. Dev.*, Report EUR, 446, 1995.

577 Dai, A.: Increasing drought under global warming in observations and models, *Nat. Clim.*
578 *Chang.*, 3(1), 52–58, doi:10.1038/nclimate1633, 2012.

579 Doerfliger, N., Jeannin, P.-Y. and Zwahlen, F.: Water vulnerability assessment in karst
580 environments: a new method of defining protection areas using a multi-attribute approach and
581 GIS tools (EPIK method), *Environ. Geol.*, 39(2), 165–176, 1999.

582 Einsiedl, F., Maloszewski, P. and Stichler, W.: Estimation of denitrification potential in a
583 karst aquifer using the ^{15}N and ^{18}O isotopes of NO_3^- , *Biogeochemistry*, 72(1), 67–86
584 [online] Available from: <http://dx.doi.org/10.1007/s10533-004-0375-8>, 2005.

585 Erisman, J. W. and Vries, W. de: Nitrogen deposition and effects on European forests,
586 *Environ. Rev.*, 8(2), 65–93, doi:10.1139/a00-006, 2000.

587 Fenicia, F., Kavetski, D., Savenije, H. H. G., Clark, M. P., Schoups, G., Pfister, L. and Freer,
588 J.: Catchment properties, function, and conceptual model representation: is there a
589 correspondence?, *Hydrol. Process.*, 28, 2451–2467, doi:10.1002/hyp.9726, 2014.

590 Feyen, L., Vrugt, J. a., Nualláin, B. Ó., van der Knijff, J. and De Roo, A.: Parameter
591 optimisation and uncertainty assessment for large-scale streamflow simulation with the
592 LISFLOOD model, *J. Hydrol.*, 332(3-4), 276–289, doi:10.1016/j.jhydrol.2006.07.004, 2007.

593 Fleury, P., Plagnes, V. and Bakalowicz, M.: Modelling of the functioning of karst aquifers
594 with a reservoir model: Application to Fontaine de Vaucluse (South of France), *J. Hydrol.*,

595 345, 38–49, 2007.

596 Ford, D. C. and Williams, P. W.: Karst Hydrogeology and Geomorphology, Wiley,
597 Chichester., 2007.

598 Fröberg, M., Jardine, P. M., Hanson, P. J., Swanston, C. W., Todd, D. E., Tarver, J. R. and
599 Garten, C. T.: Low Dissolved Organic Carbon Input from Fresh Litter to Deep Mineral Soils,
600 Soil Sci. Soc. Am. J., 71(2), 347, doi:10.2136/sssaj2006.0188, 2007.

601 Goldscheider, N. and Drew, D.: Methods in Karst Hydrogeology, edited by I. A. of
602 Hydrogeologists, Taylor & Francis Group, Leiden, NL., 2007.

603 Gough, R., Holliman, P. J., Heard, T. R. and Freeman, C.: Dissolved organic carbon and
604 trihalomethane formation potential removal during coagulation of a typical UK upland water
605 with alum, PAX-18 and PIX-322, J. Water Supply Res. Technol., 63(8), 650–660, 2014.

606 Griffin, J. M., Turner, M. G. and Simard, M.: Nitrogen cycling following mountain pine
607 beetle disturbance in lodgepole pine forests of Greater Yellowstone, For. Ecol. Manage.,
608 261(6), 1077–1089, doi:10.1016/j.foreco.2010.12.031, 2011.

609 Gundersen, P., Schmidt, I. K. and Raulund-Rasmussen, K.: Leaching of nitrate from
610 temperate forests – effects of air pollution and forest management, Environ. Rev., 14(1), 1–
611 57, doi:10.1139/a05-015, 2006.

612 Gupta, H. V., Kling, H., Yilmaz, K. K. and Martinez, G. F.: Decomposition of the mean
613 squared error and NSE performance criteria: Implications for improving hydrological
614 modelling, J. Hydrol., 377(1-2), 80–91, doi:10.1016/j.jhydrol.2009.08.003, 2009.

615 Hagedorn, F., Schleppe, P., Waldner, P. and Flühler, H.: Export of dissolved organic carbon
616 and nitrogen from Gleysol dominated catchments – the significance of water flow paths,
617 Biogeochemistry, 50, 137–161, 2000.

618 Harmon, M. E., Bond-Lamberty, B., Tang, J. and Vargas, R.: Heterotrophic respiration in
619 disturbed forests: A review with examples from North America, J. Geophys. Res.
620 Biogeosciences, 116(2), 1–17, doi:10.1029/2010JG001495, 2011.

621 Hartmann, A., Barberá, J. A., Lange, J., Andreo, B. and Weiler, M.: Progress in the
622 hydrologic simulation of time variant recharge areas of karst systems – Exemplified at a karst
623 spring in Southern Spain, Adv. Water Resour., 54, 149–160,
624 doi:10.1016/j.advwatres.2013.01.010, 2013a.

625 Hartmann, A., Gleeson, T., Rosolem, R., Pianosi, F., Wada, Y. and Wagener, T.: A large-
626 scale simulation model to assess karstic groundwater recharge over Europe and the
627 Mediterranean, Geosci. Model Dev., 8(6), 1729–1746, doi:10.5194/gmd-8-1729-2015, 2015.

628 Hartmann, A., Goldscheider, N., Wagener, T., Lange, J. and Weiler, M.: Karst water
629 resources in a changing world: Review of hydrological modeling approaches, Rev. Geophys.,
630 52(3), 218–242, doi:10.1002/2013rg000443, 2014a.

631 Hartmann, A., Kralik, M., Humer, F., Lange, J. and Weiler, M.: Identification of a karst
632 system's intrinsic hydrodynamic parameters: upscaling from single springs to the whole
633 aquifer, *Environ. Earth Sci.*, 65(8), 2377–2389, doi:10.1007/s12665-011-1033-9, 2012a.

634 Hartmann, A., Lange, J., Weiler, M., Arbel, Y. and Greenbaum, N.: A new approach to model
635 the spatial and temporal variability of recharge to karst aquifers, *Hydrol. Earth Syst. Sci.*,
636 16(7), 2219–2231, doi:10.5194/hess-16-2219-2012, 2012b.

637 Hartmann, A., Mudarra, M., Andreo, B., Marín, A., Wagener, T. and Lange, J.: Modeling
638 spatiotemporal impacts of hydroclimatic extremes on groundwater recharge at a
639 Mediterranean karst aquifer, *Water Resour. Res.*, 50(8), 6507–6521,
640 doi:10.1002/2014WR015685, 2014b.

641 Hartmann, A., Wagener, T., Rimmer, A., Lange, J., Brielmann, H. and Weiler, M.: Testing
642 the realism of model structures to identify karst system processes using water quality and
643 quantity signatures, *Water Resour. Res.*, 49, 3345–3358, doi:10.1002/wrcr.20229, 2013b.

644 Hartmann, A., Weiler, M., Wagener, T., Lange, J., Kralik, M., Humer, F., Mized, N.,
645 Rimmer, A., Barberá, J. A., Andreo, B., Butscher, C. and Huggenberger, P.: Process-based
646 karst modelling to relate hydrodynamic and hydrochemical characteristics to system
647 properties, *Hydrol. Earth Syst. Sci.*, 17(8), 3305–3321, doi:10.5194/hess-17-3305-2013,
648 2013c.

649 Heilman, J. L., Litvak, M. E., McInnes, K. J., Kjelgaard, J. F., Kamps, R. H. and Schwinning,
650 S.: Water-storage capacity controls energy partitioning and water use in karst ecosystems on
651 the Edwards Plateau, Texas, *Ecohydrology*, n/a–n/a, doi:10.1002/eco.1327, 2012.

652 Hirabayashi, Y., Mahendran, R., Koirala, S., Konoshima, L., Yamazaki, D., Watanabe, S.,
653 Kim, H. and Kanae, S.: Global flood risk under climate change, *Nat. Clim. Chang.*, 3(9), 816–
654 821, doi:10.1038/nclimate1911, 2013.

655 Högberg, M. N. and Högberg, P.: Extramatrical ectomycorrhizal mycelium contributes one-
656 third of microbial biomass and produces, together with associated roots, half the dissolved
657 organic carbon in a forest soil, *New Phytol.*, 154(3), 791–795, doi:10.1046/j.1469-
658 8137.2002.00417.x, 2002.

659 Huber, C.: Long lasting nitrate leaching after bark beetle attack in the highlands of the
660 Bavarian Forest National Park., *J. Environ. Qual.*, 34(5), 1772–9, doi:10.2134/jeq2004.0210,
661 2005.

662 Huber, C., Baumgarten, M., Göttlein, A. and Rotter, V.: Nitrogen turnover and nitrate
663 leaching after bark beetle attack in mountainous spruce stands of the Bavarian Forest National
664 Park, *Water, Air, Soil Pollut. Focus*, 4(2-3), 391–414,
665 doi:10.1023/B:WAFO.0000028367.69158.8d, 2004.

666 Humer, F. and Kralik, M.: Integrated Monitoring Zöbelboden: Hydrologische und
667 hydrochemische Untersuchungen, Unpubl. Rep. Environ. Agency, Vienna, 34, 2008.

668 Johnson, M. S., Billett, M. F., Dinsmore, K. J., Wallin, M., Dyson, K. E. and Jassal, R. S.:
669 Direct and continuous measurement of dissolved carbondioxide in freshwater aquatic systems
670 — method and applications, , 159(August 2011), 145–159, doi:10.1002/eco, 2010.

671 Jost, G., Dirnböck, T., Grabner, M.-T. and Mirtl, M.: Nitrogen Leaching of Two Forest
672 Ecosystems in a Karst Watershed, Water, Air, & Soil Pollut., 218(1-4), 633–649,
673 doi:10.1007/s11270-010-0674-8, 2010.

674 Jourde, H., Mazzilli, N., Lecoq, N., Arfib, B. and Bertin, D.: KARSTMOD: A Generic
675 Modular Reservoir Model Dedicated to Spring Discharge Modeling and Hydrodynamic
676 Analysis in Karst, in Hydrogeological and Environmental Investigations in Karst Systems SE
677 - 38, vol. 1, edited by B. Andreo, F. Carrasco, J. J. Durán, P. Jiménez, and J. W. LaMoreaux,
678 pp. 339–344, Springer Berlin Heidelberg, 2015.

679 Kaiser, K. and Kalbitz, K.: Cycling downwards - dissolved organic matter in soils, Soil Biol.
680 Biochem., 52, 29–32, doi:10.1016/j.soilbio.2012.04.002, 2012.

681 Kalbitz, K., Meyer, A., Yang, R. and Gerstberger, P.: Response of dissolved organic matter in
682 the forest floor to long-term manipulation of litter and throughfall inputs, Biogeochemistry,
683 86(3), 301–318, doi:10.1007/s10533-007-9161-8, 2007.

684 Katz, B. G., Böhlke, J. K. and Hornsby, H. D.: Timescales for nitrate contamination of spring
685 waters, northern Florida, USA, Chem. Geol., 179(1-4), 167–186, 2001.

686 Katz, B. G., Chelette, A. R. and Pratt, T. R.: Use of chemical and isotopic tracers to assess
687 nitrate contamination and ground-water age, Woodville Karst Plain, USA, J. Hydrol., 289(1-
688 4), 36–61, doi:10.1016/j.jhydrol.2003.11.001, 2004.

689 Katzensteiner, K.: Effects of harvesting on nutrient leaching in a Norway spruce (Picea, Plant
690 Soil, 250, 59–73, 2003.

691 Kiese, R., Heinzeller, C., Werner, C., Wochele, S., Grote, R. and Butterbach-Bahl, K.:
692 Quantification of nitrate leaching from German forest ecosystems by use of a process oriented
693 biogeochemical model., Environ. Pollut., 159(11), 3204–14,
694 doi:10.1016/j.envpol.2011.05.004, 2011.

695 Klemeš, V.: Dilettantism in Hydrology: Transition or Destiny, Water Resour. Res., 22(9),
696 177S–188S, 1986.

697 Kobler, J., Jandl, R., Dirnböck, T., Mirtl, M. and Schindlbacher, A.: Effects of stand
698 patchiness due to windthrow and bark beetle abatement measures on soil CO₂ efflux and net
699 ecosystem productivity of a managed temperate mountain forest, Eur. J. For. Res., 13, 683–
700 692, doi:10.1007/s10342-015-0882-2, 2015.

701 Kordilla, J., Sauter, M., Reimann, T. and Geyer, T.: Simulation of saturated and unsaturated
702 flow in karst systems at catchment scale using a double continuum approach, Hydrol. Earth
703 Syst. Sci., 16(10), 3909–3923, doi:10.5194/hess-16-3909-2012, 2012.

704 Kralik, M., Humer, F., Grath, J., Numi-Legat, J., Hanus-Illnar, A., Halas, S. and Jelenc, M.:
705 Impact of long distance air pollution on sensitive karst groundwater resources estimated by
706 means of Pb-, S-, O- and Sr-isotopes, in *Karst, cambio climático y aguas subterráneas*, edited
707 by J. J. Duran, B. Andreo, and F. Carrasco, pp. 311–317, Publicaciones del Instituto
708 Geológico y Minero de España, Serie: Hydrogeología y Aguas Subterráneas N.o 18, Madrid.,
709 2006.

710 Kralik, M., Humer, F., Papesch, W., Tesch, R., Suckow, A., Han, L. F. and Groening, M.:
711 Karstwater-ages in an alpine dolomite catchment , Austria : ^{18}O , ^3H , $^3\text{H} / ^3\text{He}$, CFC and
712 dye tracer investigations, *Geophys. Res. Abstr.*, 11, 11403, European Geosciences Union,
713 General Assembl, 2009.

714 Lindroos, A. J., Derome, J., Mustajärvi, K., Nöjd, P., Beuker, E. and Helmisaari, H. S.: Fluxes
715 of dissolved organic carbon in stand throughfall and percolation water in 12 boreal coniferous
716 stands on mineral soils in Finland, *Boreal Environ. Res.*, 13(SUPPL. B), 22–34, 2008.

717 Löfgren, S., Fröberg, M., Yu, J., Nisell, J. and Ranneby, B.: Water chemistry in 179 randomly
718 selected Swedish headwater streams related to forest production, clear-felling and climate,
719 *Environ. Monit. Assess.*, 186(12), 8907–8928, doi:10.1007/s10661-014-4054-5, 2014.

720 Mahler, B. J. and Garner, B. D.: Using Nitrate to Quantify Quick Flow in a Karst Aquifer,
721 *Ground Water*, 47(3), 350–360 [online] Available from: [http://dx.doi.org/10.1111/j.1745-](http://dx.doi.org/10.1111/j.1745-6584.2008.00499.x)
722 [6584.2008.00499.x](http://dx.doi.org/10.1111/j.1745-6584.2008.00499.x), 2009.

723 Meyer, J. L., Tate, C. M. and Feb, N.: The Effects of Watershed Disturbance on Dissolved
724 Organic Carbon Dynamics of a Stream T H E E F F E C T S O F WATERSHED
725 DISTURBANCE ON DISSOLVED, , 64(1), 33–44, 1983.

726 Michalzik, B., Kalbitz, K., Park, J., Solinger, S. and Matzner, E.: Fluxes and concentrations of
727 dissolved organic carbon and nitrogen—a synthesis for temperate forests, *Biogeochemistry*, 52,
728 173–205 [online] Available from: <http://link.springer.com/article/10.1023/A:1006441620810>,
729 2001.

730 Mikkelsen, K. M., Bearup, L. a., Maxwell, R. M., Stednick, J. D., McCray, J. E. and Sharp, J.
731 O.: Bark beetle infestation impacts on nutrient cycling, water quality and interdependent
732 hydrological effects, *Biogeochemistry*, 115, 1–21, doi:10.1007/s10533-013-9875-8, 2013.

733 Le Moine, N., Andréassian, V. and Mathevet, T.: Confronting surface- and groundwater
734 balances on the La Rochefoucauld-Touvre karstic system (Charente, France), *Water Resour.*
735 *Res.*, 44, W03403, doi:10.1029/2007WR005984, 2008.

736 Monteith, S. S., Buttle, J. M., Hazlett, P. W., Beall, F. D., Semkin, R. G. and Jeffries, D. S.:
737 Paired-basin comparison of hydrologic response in harvested and undisturbed hardwood
738 forests during snowmelt in central Ontario: II. Streamflow sources and groundwater residence
739 times, *Hydrol. Process.*, 20(5), 1117–1136, doi:10.1002/hyp.6073, 2006.

740 Neff, J. C. and Asner, G. P.: Dissolved organic carbon in terrestrial ecosystems: Synthesis and

741 a model, *Ecosystems*, 4(1), 29–48, doi:10.1007/s100210000058, 2001.

742 Perrin, J., Jeannin, P.-Y. and Zwahlen, F.: Epikarst storage in a karst aquifer: a conceptual
743 model based on isotopic data, Milandre test site, Switzerland, *J. Hydrol.*, 279, 106–124, 2003.

744 Pinault, J.-L., Pauwels, H. and Cann, C.: Inverse modeling of the hydrological and the
745 hydrochemical behavior of hydrosystems: Application to nitrate transport and denitrification,
746 *Water Resour. Res.*, 37(8), 2179–2190, 2001.

747 Raymond, P. a. and Saiers, J. E.: Event controlled DOC export from forested watersheds,
748 *Biogeochemistry*, 100(1-3), 197–209, doi:10.1007/s10533-010-9416-7, 2010.

749 Rimmer, A. and Salinger, Y.: Modelling precipitation-streamflow processes in karst basin:
750 The case of the Jordan River sources, Israel, *J. Hydrol.*, 331, 524–542, 2006.

751 Rogora, M., Mosello, R., Arisci, S., Brizzio, M. C., Barbieri, a., Balestrini, R., Waldner, P.,
752 Schmitt, M., Stähli, M., Thimonier, a., Kalina, M., Puxbaum, H., Nickus, U., Ulrich, E. and
753 Probst, a.: An Overview of Atmospheric Deposition Chemistry over the Alps: Present Status
754 and Long-term Trends, *Hydrobiologia*, 562(1), 17–40, doi:10.1007/s10750-005-1803-z, 2006.

755 Sakamoto, T., Takahashi, M., Terajima, T., Nakai, Y. and Matsuura, Y.: Comparison of the
756 effects of rainfall and snowmelt on the carbon discharge of a small, steep, forested watershed
757 in Hokkaido, northern Japan., *Hydrol. Process.*, 13(May 1998), 2301–2314,
758 doi:10.1002/(SICI)1099-1085(199910)13:14/15<2301::AID-HYP876>3.0.CO;2-U, 1999.

759 Sanderman, J., Lohse, K. a., Baldock, J. a. and Amundson, R.: Linking soils and streams:
760 Sources and chemistry of dissolved organic matter in a small coastal watershed, *Water*
761 *Resour. Res.*, 45(3), 1–13, doi:10.1029/2008WR006977, 2009.

762 Seidl, R., Schelhaas, M., Rammer, W. and Verkerk, P. J.: Increasing forest disturbances in
763 Europe and their impact on carbon storage, *Nat. Clim. Chang.*, 4(September), 1–6,
764 doi:10.1038/nclimate2318, 2014.

765 Solinger, S., Kalbitz, K. and Matzner, E.: Controls on the dynamics of dissolved organic
766 carbon and nitrogen in a Central European deciduous forest, *Biogeochem*, 55, 327–349, 2001.

767 Terajima, T. and Moriizumi, M.: Temporal and spatial changes in dissolved organic carbon
768 concentration and fluorescence intensity of fulvic acid like materials in mountainous
769 headwater catchments, *J. Hydrol.*, 479, 1–12, doi:10.1016/j.jhydrol.2012.10.023, 2013.

770 Tissier, G., Perrette, Y., Dzikowski, M., Poulénard, J., Hobléa, F., Malet, E. and Fanget, B.:
771 Seasonal changes of organic matter quality and quantity at the outlet of a forested karst
772 system (La Roche Saint Alban, French Alps), *J. Hydrol.*, 482, 139–148,
773 doi:10.1016/j.jhydrol.2012.12.045, 2013.

774 Tritz, S., Guinot, V. and Jourde, H.: Modelling the behaviour of a karst system catchment
775 using non-linear hysteretic conceptual model, *J. Hydrol.*, 397(3-4), 250–262,
776 doi:10.1016/j.jhydrol.2010.12.001, 2011.

777 Verstraeten, A., De Vos, B., Neiryneck, J., Roskams, P. and Hens, M.: Impact of air-borne or
778 canopy-derived dissolved organic carbon (DOC) on forest soil solution DOC in Flanders,
779 Belgium, *Atmos. Environ.*, 83, 155–165, doi:10.1016/j.atmosenv.2013.10.058, 2014.

780 Vrugt, J. A., Gupta, H. V., Bouten, W. and Sorooshian, S.: A Shuffled Complex Evolution
781 Metropolis algorithm for optimization and uncertainty assessment of hydrologic model
782 parameters, *Water Resour. Res.*, 39(8), 1201, doi:10.1029/2002WR001642, 2003.

783 Vrugt, J. A., Gupta, H. V., Dekker, S. C., Sorooshian, S., Wagener, T. and Bouten, W.:
784 Application of stochastic parameter optimization to the Sacramento Soil Moisture Accounting
785 model, *J. Hydrol.*, 325(1-4), 288–307, doi:10.1016/j.jhydrol.2005.10.041, 2006.

786 Weis, W., Rotter, V. and Göttlein, A.: Water and element fluxes during the regeneration of
787 Norway spruce with European beech: Effects of shelterwood-cut and clear-cut, *For. Ecol.
788 Manage.*, 224(3), 304–317, doi:10.1016/j.foreco.2005.12.040, 2006.

789 Weishaar, J. L., Aiken, G. R., Bergamaschi, B. A., Fram, M. S., Fujii, R. and Mopper, K.:
790 Evaluation of Specific Ultraviolet Absorbance as an Indicator of the Chemical Composition
791 and Reactivity of Dissolved Organic Carbon, *Environ. Sci. Technol.*, 37(20), 4702–4708,
792 doi:10.1021/es030360x, 2003.

793 WRB: World reference base for soil resources, edited by FAO, IUSS Working Group, Rome.
794 [online] Available from: <http://www.fao.org/ag/agl/agll/wrb/doc/wrb2006final.pdf>, 2006.

795 Wu, H., Peng, C., Moore, T. R., Hua, D., Li, C., Zhu, Q., Peichl, M., Arain, M. a. and Guo,
796 Z.: Modeling dissolved organic carbon in temperate forest soils: TRIPLEX-DOC model
797 development and validation, *Geosci. Model Dev.*, 7(3), 867–881, doi:10.5194/gmd-7-867-
798 2014, 2014.

799 Wu, Y., Clarke, N. and Mulder, J.: Dissolved Organic Nitrogen Concentrations and Ratios of
800 Dissolved Organic Carbon to Dissolved Organic Nitrogen in Throughfall and Soil Waters in
801 Norway Spruce and Scots Pine Forest Stands Throughout Norway, *Water, Air, Soil Pollut.*,
802 210(1-4), 171–186, doi:10.1007/s11270-009-0239-x, 2009.

803

804

805 **10 Table captions**

806 Table 1: model parameters, description, ranges and calibrated values with *KGE* performances
807 for the calibration and validation samples

808 Table 2: calibrated pre-storm parameters for DIN dynamics and 2 scenarios for adapting it at
809 the stormy period

810 **11 Figure captions**

811 Figure 1: study site and location of measurement devices (Hartmann et al., 2012a; modified).

812 Figure 2: Intra-annual and inter-annual variations of (a) DOC concentrations, (c) DIN
813 concentrations and (e) discharge, and relation between discharge and (b) DOC and (d) DIN
814 before and during the wind disturbance period.

815 Figure 3: Sketch of model structure; it is assumed that discharge and hydrochemistry at the
816 two weirs is composed by different mixtures of diffuse recharge (green), concentrated
817 recharge (red), diffuse groundwater flow (blue) and concentrated groundwater flow (purple)

818 Figure 4: Observed versus simulated discharges for the entire karst system and weir 1
819 Figure 4: Observed versus simulated discharges for the entire karst system and weir 1
820 Figure 5: Observed versus simulated (a) DOC and (b) DIN at weir 1.

821 Figure 5: Observed versus simulated (a) DOC and (b) DIN at weir 1.

822 Figure 6: Individual components of the *KGE*: (a) ratio of simulated and observed variabilities,
823 (b) ratio of simulated and observed average values, and (c) their correlation for the wind
824 disturbance period; for comparison the *KGE* components and their inter-annual variability are
825 also shown for pre-storm period and after the correction of the DIN production model
826 parameters during the wind period.

827 Figure 7: Observed and simulated DIN dynamics using the pre-storm parameters (red line),
828 the scenario 1 parameters derived from the deviations assessed by the *KGE* components
829 (orange line), and the scenario 2 parameters derived by systematic variation (dark red line).

830 Figure 8: Mean transit times for (a) the soil and epikarst and (c) the groundwater storages
831 derived by an infinite virtual tracer injection starting with the beginning of the wind
832 disturbance period, and the reaction of (b) the soil and epikarst, and (d) the groundwater
833 storage as the impact ends.

834 **12 Tables**835 **Table 1: model parameters, description, ranges and calibrated values with *KGE* performances for the**
836 **calibration and validation samples**

Parameter	Description	Unit	Ranges		Optimized values	
			Lower	Upper	Sample 1	Sample 2
$V_{mean,S}$	Mean soil storage capacity	mm	0	1500	450.18	599.13
$f_{var,S}$	fraction of the spoil that has a variable depth	-	0	1	0.06	0.02
$V_{mean,E}$	Mean epikarst storage capacity	mm	0	1500	1495.49	1233.98
α_{SE}	Soil/epikarst depth variability constant	-	0	2	1.69	1.91
$K_{mean,E}$	Epikarst mean storage constant	d	1	50	2.65	8.27
α_{sep}	Recharge separation variability constant	-	0	2	0.88	1.44
K_C	Conduit storage constant	d	1	10	1.37	1.03
α_{GW}	Groundwater variability constant	-	0	2	2.00	1.88
f_{EW}	Fraction of weir discharge originating from the epikarst	-	0	1	0.56	0.72
$f_{WE,conc}$	Fraction of weir discharge originating from the epikarst as concentrated flow	-	0	1	0.57	0.47
$f_{WGW,conc}$	fraction of weir discharge originating from the groundwater as concentrated flow	-	0	1	0.01	0.06
P_{DOC}	DOC production parameter	mg l ⁻¹	0	15	1.79	1.57
α_{DOC}	DOC variability constant	-	0	2	0.92	1.05
P_{DIN}	DIN production parameter	mg l ⁻¹	-5	10	-1.35	0.11
$S_{PH,DIN}$	Phase of annual DIN production	d	0	365	0	2
A_{DIN}	Amplitude of annual DIN production	mg l ⁻¹	0	10	3.36	1.84
$G_{max,SO4}$	Equilibrium concentration of SO ₄ in matrix	mg l ⁻¹	0	50	2.74	3.07
α_{Geo}	Equilibrium concentration variability constant	-	0	2	0.11	0.04
$KGE_{weighted}$	weighted multi-objective model performance	-	0	1	0.56/0.49*	0.52/0.53*
$KGE_{Q,tot}$	model performance for discharge of entire system	-	0	1	0.41/0.33*	0.35/0.42*
$KGE_{Q,W}$	model performance for discharge of weir	-	0	1	0.67/0.62*	0.61/0.66*
KGE_{DOC}	model performance for DOC concentrations	-	0	1	0.38/0.35*	0.43/0.32*
KGE_{DIN}	model performance for NO ₃ concentrations	-	0	1	0.48/0.40*	0.48/0.45*
KGE_{SO4}	model performance for SO ₄ concentrations	-	0	1	0.74/0.62*	0.64/0.65*

837 * calibration/validation with other sample

838

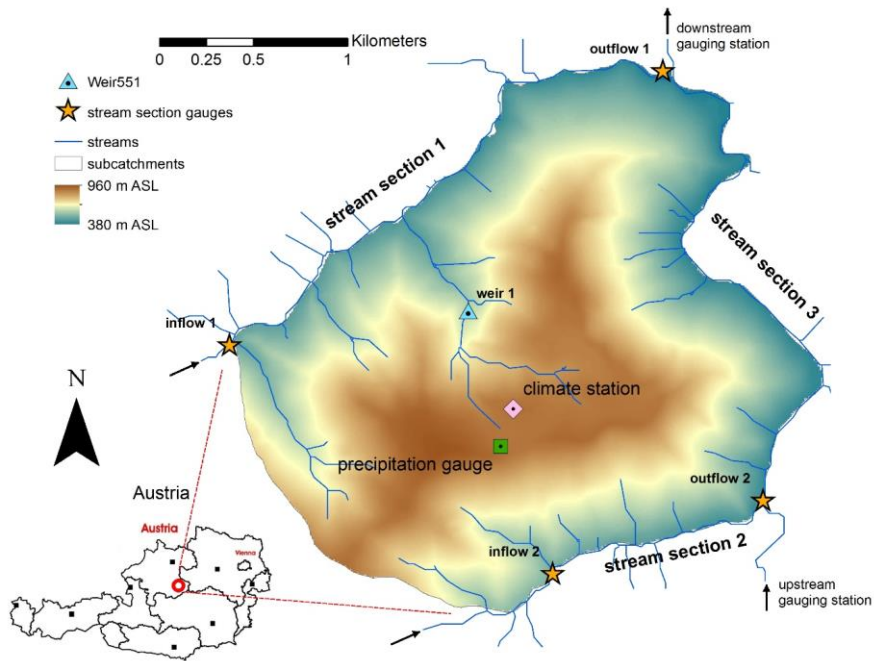
839 **Table 2: calibrated pre-storm parameters for DIN dynamics and 2 scenrios for adapting it at the stormy**
840 **period**

Parameter	Unit	Calibration type		
		Pre-storm	manual	automatic
P_{DIN}	mg l ⁻¹	0.11	2.10	0.00
$S_{PH,DIN}$	d	2.00	9.00	23
A_{DIN}	mg l ⁻¹	1.80	0.70	2.63
KGE_{DIN}^*	-	0.29	0.41	0.46
variability α_{DIN}^*	-	0.75	1.04	1.05
bias β_{DIN}^*	-	0.70	1.01	0.83
correlation $_{DIN}^*$	-	0.40	0.41	0.49

* for 2006/07-2011/12

841

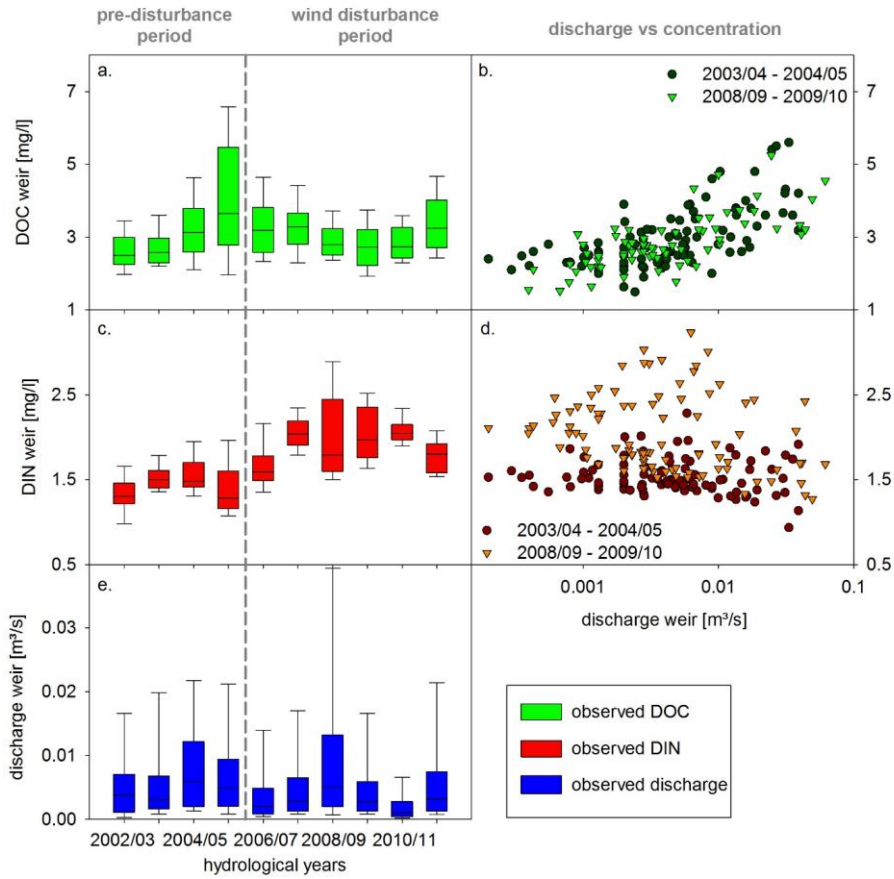
842 **13 Figures**



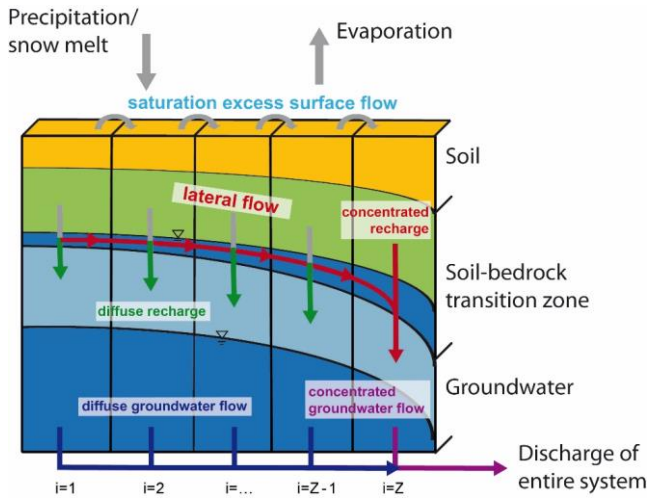
843

844 **Figure 1: study site and location of measurement devices (Hartmann et al., 2012a;modified).**

845

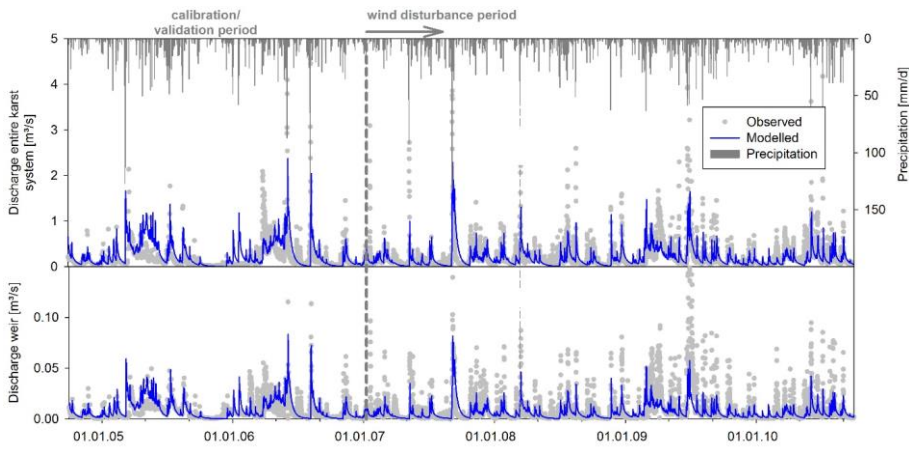


846
 847 **Figure 2: Intra-annual and inter-annual variations of (a) DOC concentrations, (c) DIN concentrations and**
 848 **(e) discharge, and relation between discharge and (b) DOC and (d) DIN before and during the wind**
 849 **disturbance period.**
 850



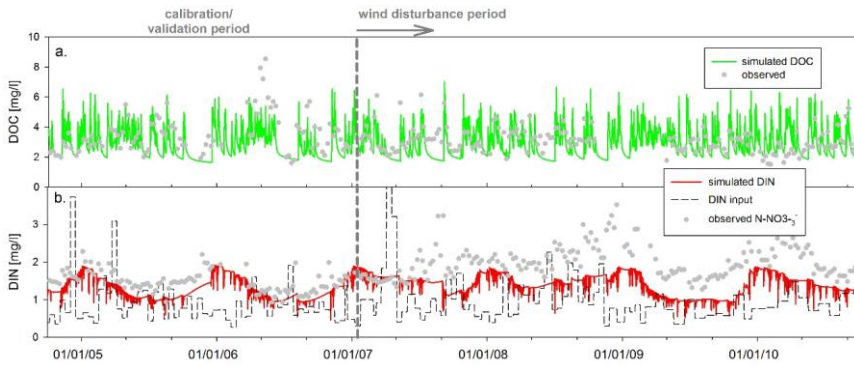
851
 852 **Figure 3: Sketch of model structure; it is assumed that discharge and hydrochemistry at the two weirs is**
 853 **composed by different mixtures of diffuse recharge (green), concentrated recharge (red), diffuse**
 854 **groundwater flow (blue) and concentrated groundwater flow (purple)**

855



856
 857 **Figure 4: Observed versus simulated discharges for the entire karst system and weir 1**

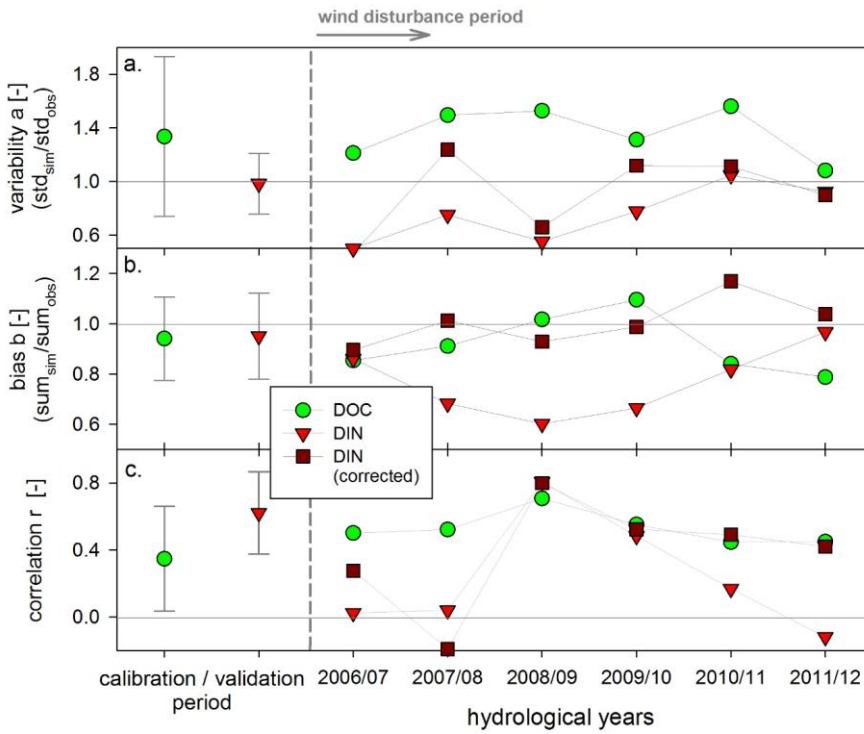
858



859

860 **Figure 5: Observed versus simulated (a) DOC and (b) DIN at weir 1.**

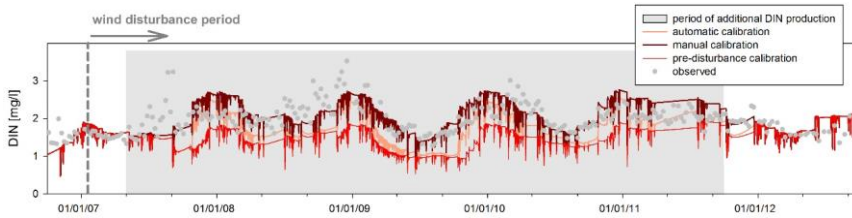
861



862

863 **Figure 6: Individual components of the KGE: (a) ratio of simulated and observed variabilities, (b) ratio of**
 864 **simulated and observed average values, and (c) their correlation for the wind disturbance period; for**
 865 **comparison the KGE components and their inter-annual variability are also shown for pre-storm period**
 866 **and after the correction of the DIN production model parameters during the wind period.**

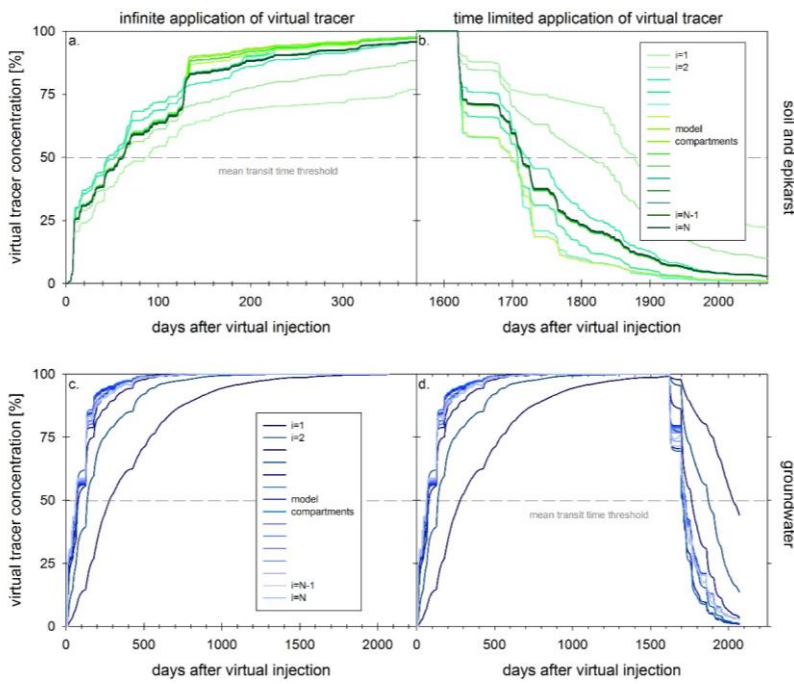
867



868

869 **Figure 7: Observed and simulated DIN dynamics using the pre-storm parameters (red line), the scenario 1**
870 **parameters derived from the deviations assessed by the KGE components (orange line), and the scenario 2**
871 **parameters derived by systematic variation (dark red line).**

872



873

874 **Figure 8: Mean transit times for (a) the soil and epikarst and (c) the groundwater storages derived by an**
875 **infinite virtual tracer injection starting with the beginning of the wind disturbance period, and the**
876 **reaction of (b) the soil and epikarst, and (d) the groundwater storage as the impact ends.**